The role of axial ligands for the structure and function of chlorophylls

Heimdal, Jimmy; Jensen, Kasper; Devarajan, Ajitha; Ryde, Ulf

Published in:
Journal of Biological Inorganic Chemistry

DOI:
10.1007/s00775-006-0164-z

2007

Document Version:
Peer reviewed version (aka post-print)

The role of axial ligands for the structure and function of chlorophylls

Jimmy Heimdal, Kasper P. Jensen, Ajitha Devarajan, Ulf Ryde *

Department of Theoretical Chemistry, Lund University, Chemical Centre, P. O. Box 124, SE-221 00 Lund, Sweden

Correspondence to Ulf Ryde, E-mail: Ulf.Ryde@teokem.lu.se, Tel: +46 – 46 2224502, Fax: +46 – 46 2224543

2017-03-19

Non-standard abbreviations: BChl – bacteriochlorophyll, BDE – bond dissociation energy, Chl – chlorophyll, LCH – light-harvesting complex, Pheo – pheophytin,PSI – photosystem I, PSII – photosystem II, RC – reaction centre, RI – resolution-of-the-identity approximation.

We have studied the effect of axial ligation of chlorophyll and bacteriochlorophyll using density functional calculations. Eleven different axial ligands have been considered, including models of His, Asp/Glu, Asn/Gln, Ser, Tyr, Met, water, the protein back-bone, and phosphate. The native chlorophylls, as well as their cation and anion radical states and models of the reaction centres P680 and P700, have been studied and we have compared the geometries, binding energies, reduction potentials, and absorption spectra. Our results clearly show that the chlorophylls strongly prefer to be five-coordinate, in accordance with available crystal structures. The axial ligands decrease the reduction potentials, so they cannot explain the high potential of P680. They also red-shift the *Q* band, but not enough to explain the occurrence of red chlorophylls. However, there is some relation between the axial ligands and their location in the various photosynthetic proteins. In particular, the intrinsic reduction potential of the second molecule in the electron-transfer path is always lower than that of the third one, a feature that may prevent the back-transfer of the electron.

Keywords: chlorophyll, photosynthesis, axial ligands, density functional theory, reduction potential

Introduction

Photosynthesis serves as the direct or indirect energy source for all higher life on earth. The photosynthetic conversion of solar energy to chemical energy is strongly associated with chlorophyll (Chl) or bacteriochlorophyll (BChl), because they take part in both the light-harvesting process and the energy conversion [1,2]. The photosynthetic apparatus in higher plants contains two complexes, photosystems I and II (PSI and PSII), in which the fundamental reactions of photosynthesis take place. They are associated with light-harvesting complexes (LHC), which take part in the distribution of excitation energy between PSI and PSII [3,4].

The chemical process in photosynthesis is based on the reaction

$$H_2O + CO_2 + h\boxed{?}\ \boxed{?}\ (CH_2O) + O_2 \qquad (1)$$

where $h\boxed{?}$ represents the photons of light and (CH_2O) represents carbohydrates (biomass). The reaction is very energy-consuming (ΔH = +470 kJ/mole [2]), which explains the complexity of the photosynthetic system. The sunlight that reaches the surface of earth spans all wavelengths in the visible region (380–750 nm), but also higher wavelengths, up to over 1000 nm. However, this energy (120–315 kJ/mole) is not enough to drive the photosynthetic process. Therefore, the energy from several photons has to be accumulated. This is done by a variety of organic pigments, including chlorophylls. Chlorophylls have two strong absorption bands around 680 and 450 nm, which give them their well-known green colour.

The chlorophylls consist of a tetrapyrrole ring with a Mg^{2+} ion in the centre (Figure 1). One (Chl, ring IV) or two (BChl, also ring II) bonds in the tetrapyrrole ring are reduced compared to a normal porphyrin and one of the pyrrole rings (III) is fused with a cyclopentanone ring. In addition, several of the side chains are different from those of haem. In particular, one of the substituents is a long phytol ester. There are several variants of Chl, which differ in the side chains, e.g. Chl *a* and *b* (Figure 1).

In addition to the four ligands in the chlorophyll ring, the Mg ion may have an axial ligand from the surrounding protein, but the ligand varies a lot, depending on the protein. In

Table 1, we provide a survey of axial ligands in the LHC from spinach and in PSI and PSII from a cyanobacterium [4,5,6]. From this, it can be seen that most chlorophylls are five-coordinate: Only a single site is six-coordinate (and this is probably an artefact, see below), and a few sites have a second ligand at a seemingly non-bonded distance (>339 pm). A small number of the chlorophylls are four-coordinate without axial ligands: 0–2% in the two proteins at moderate resolution and 17% in the low-resolution (350 pm) structure of PSII, where no water molecules are recognised. The dominating ligand in the two photosystems is histidine (His, 68–75%), whereas in the LHC water, carboxylates, and amides are equally common (14–29%). The significance of this variation in the axial ligation is not clear.

The reaction centre (RC) of PSII is called P680 (a pigment with the absorption maximum at 680 nm). It is a Chl *a* dimer, with a Mg–Mg distance of 820 pm and each Mg axially ligated by a His residue [6]. Upon photon absorption, an electron is released and quickly transferred via a Chl *a* molecule (the accessory Chl) and one pheophytin molecule (chlorophyll without the central Mg ion) to the final electron acceptor, a plastoquinone. In this process, PSII obtains a very high positive potential that is used for the oxidation of two water molecules to dioxygen in the oxygen-evolving complex. The plastoquinone molecule diffuses to the cytochrome *bf* complex, where the electron is transferred to a molecule of plastocyanin and ATP is synthesised. Plastocyanin, finally, transports the electron to PSI. The structures of P680 and the electron transfer pathways are very similar to the bacterial equivalent of PSII (called P960), the only differences being that the BChls of the special pair are closer together and the accessory BChl *a* is also ligated by His.

The primary electron donor in PSI is called P700. It is also a chlorophyll dimer, composed of a Chl *a* molecule and the $C13^2$ epimer of Chl *a* (Chl *a*') [5]. They are both ligated by His. There are two additional Chl *a* molecules in the electron-transfer pathway. The first is ligated by water (Chl-w) and the second by methionine (Chl-m). Spectroscopic measurements indicate that Chl-m is the electron acceptor, whereas Chl-w only mediates the electron transfer from P700 to Chl-m [7]. The ultimate electron acceptor in PSI is ferredoxin, which transports

the electron to NADP reductase, where it is used in the synthesis of NADPH.

Considering the importance of Chl and BChl in photosynthesis, it is not unexpected that a large number theoretical studies have been devoted to these systems, using a variety of different methods, viz semiempirical, ab initio, combined quantum mechanical and molecular mechanics, molecular dynamics, and density functional theory [e.g. 8,9,10,11]. A number of properties have been studied, e.g. spectroscopy, electronic structure, ionisation potential, and electron transfer. However, only a few papers discuss the effect of axial ligands and only for specific cases and properties. For example, some groups have included all protein residues within 250–700 pm of the chlorophyll in spectral calculations of specific proteins, which sometimes involves an axial ligand [8,12,13,14,15], but the actual effect of the ligand was not studied. Likewise, studies of the reaction centres of the two photosystems have involved the axial His ligands [16,17,18,19,20]. Moreover, several groups have included one or two water molecules in studies of the spectra and reduction potentials of various chlorophylls [8,21,22,23,24,25,26]. However, only in a few papers has the actual effect of the axial ligation on the structure, spectrum, and reduction potentials been studied (for water, histidine, and a N-terminal formyl group) [8,26,27,28].

Given the variation of the axial ligands, it is important to clarify their influence in a more systematic way. Therefore, we have performed an investigation of the effect of all types of axial ligation to Chl and BChl observed in the survey in Table 1. We study how the axial ligands change the structure, spectroscopy, and reduction potentials of the chlorophylls and also the strength of the binding. This investigation also allows us to discuss the construction and design of the photosystems and light-harvesting complexes.

Methods

Chlorophyll (Chl) and bacterial chlorophyll (BChl) were modelled as the tetra-pyrrole backbone with a cyclopentanone ring attached to ring III, but without any side chains, as is shown in Figure 2. The only difference between the models of Chl and BChl is the saturated

bond in ring II in BChl. Since the side chains were omitted, the present model is a mimic of (B)Chl *a* as well as *b*, because they differ in the nature of one of the side chains (cf. Figure 1).

Test calculations were also performed on 13 models including all side chains (including models of both Chl *a*, Chl *b*, and BChl *a*), except that the phytol chain was truncated either after the first ethyl group or after $–CH_2CH_2COOCH_3$. These calculations showed that inclusion of the side chains change the geometry around the Mg ion by less than 2 pm, absolute bond dissociation energies by up to 8 kJ/mole in vacuum and 3 kJ/mole in water solution, but the relative values (for different axial ligands) by less than 2 kJ/mole. Likewise, the absolute reduction potentials change by up to 0.4 V in vacuum and 0.1 V in water solution, but the relative values by less than 0.06 and 0.02 V in vacuum and water solution, respectively. Therefore, we can safely ignore the chlorophyll side chains in this comparative investigation.

Eleven different axial ligands were considered, namely water (H_2O), CH_2CONH_2 as a model of aspargine (Asn), CH_2COO^- for aspartate (Asp), $CH_3CONHCH_3$ for an amino-acid back-bone (Backb), imidazole for histidine (His), CH_3SCH_3 for methionine (Met), $[CH_3OPO_2OCH_3]^-$ for phosphate (Phos), CH_3OH as a model of an alcohol, e.g. in serine (Ser), and a phenol group as a model of tyrosine (Tyr). Calculations were also performed with a deprotonated alkoxide (Ser^-) and a six-coordinate system with two histidine ligands (2His). These are the axial ligands observed in the survey in Table 1. The 2His system was included in an attempt to understand why Mg is not six-coordinate in the proteins, using the most common ligand, His, as an example.

We also tested the strange six-coordinated structure of Chl-34 and 2034 in PSII, which has both a His ligand and an ethyl group from a neighbouring Chl (with a Mg–C distance 246 pm). However, after optimisation of such a structure, the Mg–C distance increased to 485 pm, i.e. close to the distance in the newer PSII structure at 300 pm resolution [29]. Therefore, we strongly believe that this strange interaction is an artefact of the low resolution of that structure and we do not consider it further in this paper.

For all models, the doublet cation radical and the doublet anion radical, formed by removing or adding an electron to the models, were also studied. Although removal (addition) of an electron from the negatively charged systems (Asp, Ser^{-}, and Phos) gives a neutral (doubly anionic) structure, we will adopt the name cation (anion) radical throughout the text for these species.

Geometry optimisations where performed with density-functional theory using Becke's 1988 gradient corrected exchange functional, combined with Perdew's 1986 correlation functional (BP86) [30,31]. The 6-31G* basis set where used for all atoms [32]. To speed up the calculations, Coulomb operators were treated using the resolution-of-identity (RI) approximation (the electron density is approximated by an expansion in atom-centred auxiliary basis sets, which avoids the calculation of four-centre two-electron integrals) [33,34]. This reduces the computational cost by a factor 4–10.

After the geometry optimisations, accurate energies were calculated using the three-parameter hybrid functional B3LYP, as implemented in the TURBOMOLE software [35]. For these calculations, the 6-311+G(2d,2p) basis set was used for all atoms.

In order to better understand the effect of solvation on the relative energies of the various systems, we have also calculated (single-point) solvation energies using the continuum conductor-like screening model (COSMO) as implemented in Turbomole [36,37]. These calculations were performed at the BP86/6-31G* level, with default values for all parameters (implying a water-like probe molecule) and with a dielectric constant (ε) of 80 and 4, to model pure water and to evaluate possible effects in a protein (where the effective dielectric constant is normally estimated to be 2–16 [38,39]). For the generation of the cavity, a set of atomic radii has to be defined. We used the optimised COSMO radii in Turbomole (H: 130, C: 200, N: 183, O: 172, S: 216, P: 200, and Mg: 200 pm) [40]. The solvation energy (energy difference between solvation and vacuum calculations with the same method) was added to the B3LYP/6-311+G(2d,2p) energies.

Reduction potentials were estimated by

$$E_0 = E(\text{oxidised state}) - E(\text{reduced state}) - 4.43 \quad (2)$$

where the factor 4.43 eV is an estimate of the potential of the standard hydrogen electrode [41].

Likewise, binding strengths of the various ligands to the ligand-free (B)Chl was estimated as the Mg–ligand bond dissociation energy (BDE), calculated from the B3LYP and COSMO energies:

$$BDE = E(\text{complex}) - E(\text{Chl}) - E(\text{ligand}) \quad (3)$$

Time-dependent density-functional theory [42,43] was used to calculate single-state excitations for all the systems. This was done with BP86 functional and the RI approximation. The TZVPP basis set was used [44] and the 21 lowest states were considered. In these calculations, we employed stricter convergence criteria than default, scfconv = 8 and rpaconv = 7 (default values 6 and 5, respectively). Such a method has repeatedly been shown to give acceptable electronic spectra of similar systems at a reasonable time consumption [45,46], even if it has been shown that the method predicts many dubious charge-transfer states with low intensity [43,47]. Since we study only the two most intense peaks in the spectra, these problems should not affect the results significantly.

Result and Discussion

Geometries

We have studied the effect of axial ligation in Chl and BChl for a number of different properties. First, we study their effect on the geometric and electronic structures. The optimised structure of Chl without any axial ligand is shown in Figure 2. It can be seen that the Mg ion is in the plane of the chlorophyll ring. However, the Mg–N distances are not equal, as can be seen from Table 2: The Mg–N4 bond (to ring IV; 217 pm) is 14 pm longer than that to ring III (203 pm), and that to ring II is also elongated (208 pm). The reason for this is the saturated bond in ring IV.

All the axial ligands coordinate to the Mg ion. The Mg–ligand bond length depends strongly on the ligand. It is 190–199 pm for the three negatively charges ligands (Ser^-, Asp, and Phos, in this order) and 210–221 pm for the neutral ligands (Backb < Asn < Ser < H_2O < Tyr < His. The bonds are even longer in the complex with two His ligands (235 pm) and especially in the Met complex (274 pm).

The optimised distances are fairly similar to those in the crystal structures (Table 1), but there is a very large variation in the latter, owing to the low resolution of the crystal structures. However, it is notable that for many ligands (Ser, Backb, Phos, and Asp), the optimised distances are shorter than any of the experimental distances. The reason for this is probably that no bonds were defined between the Mg ion and the ligand in the crystallographic refinement, meaning that the distances are restrained towards the van der Waals minimum between the two groups, which is typically around 250 pm [48]. For low-resolution structures, where the electron density is poorly defined, such restraints have a strong influence on the final distance. However, for the alcohols (and the back-bone interactions in PSII), it is clear that there is no direct bond between the ligand and Mg in the proteins (distances 339–370 pm). In particular, it is clear that the alcohols are not deprotonated (cf. Ser^-).

When axial ligands are added to Chl, all the Mg–N bonds are elongated, by 2–4 pm for the neutral ligands and by 7–11 pm for the negatively charged ligands. All the bonds are elongated by approximately the same amount so the Mg–N4 bonds remains 12–17 pm longer than the shortest Mg–N bond. In addition, the coordination of an axial ligand leads to a displacement of the Mg ion out of the Chl ring plane towards the axial ligand: 57–68 pm for the negatively charged ligands and 26–40 pm for the neutral ligands (in the complex with two His ligands, the Mg ion remains in the ring plane).

When an electron is removed from the models (yielding the cation radicals), the Mg–N distances change by less than 2 pm and the distances to the axial ligand shorten by 3–5 pm, as can be seen in Table 3. As a consequence, the out-of-plane distances increase, typically by ~8 pm. There are two exceptions to this general trend, Ser^- and Asp, for which all Mg–N

distances shorten by ~4 and 0–2 pm and the axial ligand moves away from Mg by 7 and 1 pm, respectively. The out-of-plane distances also decrease by 15 and 5 pm, respectively. The unpaired electron resides entirely in the Chl ring (less than 0.01 unpaired electrons on Mg and the ligand) in all complexes, except the Ser^- and Asp complexes, which have 0.42 and 0.23 unpaired electrons on the ligands, respectively. This explains the diverging behaviour of the two latter complexes.

When an electron is instead added to the models to get the Chl anion radicals, similar trends are observed as for the cation radicals, but Ser^- and Asp no longer differ from the other ligands: Table 3 shows that the Mg–N distances change by less than 3 pm. Typically, the two long bonds (to N2 and N4) are shortened and those to the short bonds are elongated, making the difference smaller. However, upon reduction, the distance to the axial ligand are elongated by 1–7 pm and therefore, the out-of-plane distances shorten (by 0–7 pm). The radical is located entirely in the Chl ring for all complexes. The Tyr complex shows somewhat larger changes, owing to a slight reorientation of the phenol ring.

We have also performed the corresponding calculations for the BChl complexes with the same axial ligands. The results are collected in Tables 4 and 5. The optimised structure of BChl is similar to that of Chl. However, the Mg–N2 distance (215 pm) is almost as long as the Mg–N4 distance, because in BChl, also ring II is saturated. Moreover, the Mg–N4 distance is still 1–5 pm longer, showing that the cyclopentanone ring also has some influence on the distances. This behaviour remains when axial ligands are added. All the other distances (including that of the axial ligand and the out-of-plane distances) differ by less than 3 pm from the corresponding Chl complex. Likewise, the changes in distances when an electron is added or removed are very similar for Chl and BChl. Thus, we can conclude that the choice of the chlorophyll ring and the axial ligand only have a modest effect on the equatorial ligand field and overall structure.

Bond strengths

From the survey in Table 1, it is clear that the great majority of chlorophylls in proteins are five-coordinate. This is in conspicuous contrast to haem, for which six-coordination is frequently seen (e.g. all cytochromes) [2]. In order to understand this difference, we have studied the intrinsic strength of the bond between the axial ligands and Mg in Chl and BChl, as measured by the bond dissociation energy (BDE) of the Mg–ligand bond (defined in Eqn. 3). The results in Table 6 show that it is positive for all ligands. It is 28 kJ/mole for Met, 36–70 kJ/mole for the other neutral ligands (Tyr < H_2O < Ser < Asn < Backb < His), 84 kJ/mol for 2His, and 170–260 for the negatively charged ligands (Phos < Asp < Ser^-). From Table 2, it can be seen that the BDE is quite well correlated to the Mg–ligand bond distance, with one conspicuous exception: His has a longer Mg–ligand distance than H_2O, but a much higher BDE. This is even more evident for 2His. From an inorganic point of view, it is also somewhat unexpected that the hard Mg^{2+} ion binds the rather soft His ligand stronger than the hard O-ligands (and also that it binds the very soft Met ligand at all) [2].

The BDE is reduced in the solvents, especially for 2His (for which the BDE becomes lower than for one His) and the negatively charged ligands (which become less strongly bound than Asn), but it is still positive for all ligands. The binding is typically a few kJ/mole stronger to BChl than to Chl (4 kJ/mole on average).

It should be noted that these bond strengths are highly approximate, because both the basis-set superposition error, zero-point energy, and entropic effects have been ignored. Their inclusion would all decrease the strength of the binding, typically by 30–70 kJ/mole [49,50] (thermal effects are also ignored but they are normally much smaller, ~6 kJ/mole [50]). Of course, the binding is also determined by the available alternative binding sites for the ligands in the protein. All ligands except Met can form hydrogen bonds by the ligating atom, the strength of which are of a similar magnitude as the calculated bond strengths to the Mg ion. Therefore, the absolute values of all these bond strengths are very uncertain, but the relative values can be more trusted.

We can conclude that the BDE of the first axial ligands to Chl and BChl is quite normal: For example, the corresponding BDEs of His and Asn ligands to Co(II)corrin are 85–52 and 72–35 kJ/mole (? = 1–80) [51] and the binding energy of water to Fe(II)porphine is 57–40 kJ/mole [52], i.e. similar to what is found for Chl and BChl. However, the binding of a second ligand to (B)Chl is much weaker than normal: In fact, there is no gain in binding energy of the second ligand in the two solvent models. In contrast, the binding of a second His ligand or a second water molecule to Fe(II)(porphine) is 51–23, and 48–20 kJ/mole (? = 1–80), respectively [52,53]. This clearly explains why six-coordinate Chl molecules are not encountered in the proteins.

Reduction potentials

Many of the processes in photosynthesis involve the transfer of electrons. The driving force for such reactions is determined by the reduction potential. Therefore, we have investigated the effect of axial ligation on the reduction potential for our Chl and BChl models. The reduction potentials of the cationic radical of Chl and BChl, calculated from the B3LYP and COSMO energies, are listed in Table 7. In general, the potentials decrease when an axial ligand is added, showing that the axial ligand stabilises the oxidised state. Quite naturally, the effect is largest for the negatively charged ligands Asp, Phos, and Ser^{-}, for which the potential decreases by ~3 V. The potentials follow the same order as the BDEs, except for His: Met ? Tyr > H_2O ? Ser > His > Asn ? Backb > 2His >> Phos ? Asp ? Ser. Solvation effects reduce the differences, and in water solution, all complexes have the same potential within 0.2 V, but the complex without any axial ligand still has the highest potential. The calculated result for Chl without any axial ligand (1.11 V, ε = 4 and 0.64 V, ε = 80; 1.16 and 0.76 V with side chains) is close to the experimental one, 0.93 V in tetrahydrofuran (ε = 7.6) [54]. The reduction potentials of the BChl species are ~0.45 V lower than those of the corresponding Chl complexes, but they exhibit the same trends as for Chl.

The reduction potentials of neutral Chl and BChl, giving the anion radicals, are ~2.8 V

more negative in a protein-like environment than those of the cation radicals (~1.8 V in water), and the potentials of BChl are only ~0.02 V more negative than that of Chl (Table 8). The trends are similar to those of the cations. Solvation effects reduce these differences and in water solution, all potentials are the same within 0.2 V, again with the complex without any axial ligand giving the least negative potential.

Pheophytin (Pheo) is an important molecule in photosynthetic reactions, being involved in the electron transfer pathway in PSII. This makes its redox properties interesting: The calculated potentials of Pheo are ~0.1 V more positive than those of Chl without any axial ligand. The calculated potential of the Pheo/Pheo$^+$ pair (1.23 in $\varepsilon = 4$, 0.79 in $\varepsilon = 80$; 1.06 and 0.70 V for Pheo *a* with side chains) agrees reasonably well with the experimental one, 0.70 V in butyronitrile ($\varepsilon = \sim 21$) [42].

The special pair of the reaction centres of the various photosystems is known to have a high positive potential for the RC$^+$/RC couple (~1.2 V for P680$^+$, but ~0.4 V for P700$^+$) [2]. On the other hand, the potential for the excited state RC*/RC^{*+} should be much more negative (–0.9 V for P680^{*+} and –1.1 V for P700^{*+}) [54]. We have included a simple dimeric model of P700 in our calculations (two Chl rings without any side-chains but with axial His ligands; Figure 3). Using the crystal structure, the P700$^+$/P700 reduction potential is 1.4–0.4 V (ε = 1–80) with the two axial His ligands, observed in the crystal structure, and 0.2–0.5 V higher without them. The former result is quite close to the experimental estimate for P700$^+$ (~0.4 V). The result indicates that the dimer has a lower reduction potential than all the monomers, except those with negatively charged ligands. As for the monomers, the axial ligands decrease the reduction potential.

We have also done similar calculations on P680, the RC in PSII. The same model as for P700 was used; the only difference is the coordinates, which were taken from the crystal structure [5,6]. The results in Table 7 show that we predict a slightly higher potential for this site, but only by 0.1–0.2 V, compared to the experimental estimate of 0.8 V. Thus, our calculations give no clue to how the very high potential of P680$^+$ is obtained (~1.2 V). Such a

high potential is only obtained in a very hydrophobic environment ($\varepsilon < 4$; as has been noted before [55]) and preferably for Pheo or a Chl monomer without any axial ligands. A dimer with His ligands is predicted to give lower potentials. It is likely that the potential of $P680^+$ is tuned by electrostatic effects in the protein.

In PSI, the electron path consists of P700, a Chl *a* molecule ligated by water, followed by a Chl *a* ligated by methionine. This choice of axial ligands is appropriate: The calculated reduction potential of a neutral Chl is more negative if the axial ligand is water than if it is methionine (e.g –1.87 compare to –1.79 V at $\varepsilon = 4$). This means that the electron transport from the Chl ligated by water to that ligated by methionine is favourable in energy terms. It has been proposed that this is a mechanism to prevent back-transfer of electrons [26].

In the PSII reaction centre, the reactive species in the electron transfer pathway are P680, Chl *a*, and Pheo. The latter two show the same trend in reduction potentials as the corresponding pathway in PSI: The second molecule in the pathway has a slightly more negative reduction potential than the third one, Chl –1.69 V and Pheo –1.53 V ($\varepsilon = 4$), i.e, a difference of 0.16 V (and possible axial ligands to the Chl will only increase the difference). Likewise, in the bacterial RC the two first molecules of the electron transfer pathway are a BChl *a* ligated by an axial histidine and a Pheo molecule: The potential of the BChl molecule is predicted to be 0.37 V more negative than that of Pheo.

Consequently, although there are structural differences between the electron transfer pathways of PSI, PSII, and BRC and they can be tuned in different ways by electrostatic interactions with the surrounding protein, they all share a common feature, viz. that the intrinsic reduction potential of the second molecule in the electron-transfer pathway always is more negative than that of the third one. This makes the forward transfer of an electron energetically favourable, whereas the back-transfer of the electron is an uphill reaction. Even if the estimated energy differences are not very large (0.08–0.37 eV), this corresponds to reaction half-times of 4 ps to 300 ns (ignoring any other contributions to the activation energy that would increase the reaction time), which are significant compared measured electron

transfer rates, e.g. 3 and 1 ps for the first two steps for the bacterial reaction centre.[2]

Absorption spectra

Finally, we have studied the effect of axial ligation on the absorption spectra of chlorophyll. As mentioned in the methods section, we have calculated the 21 lowest excitation energies for each complex. However, to make the discussion clear, we have concentrated on only two bands, viz, the two most intense bands at a low energy. They are found at 598 and 343 nm for Chl and 657 and 341 nm for BChl. They correspond to the most intense peaks of the *Q* (Q_y) and *B* (Soret) bands in the experimental spectra, observed at 660 and 428 nm for Chl *a*, at 642 and 452 nm for Chl *b*, and at 795 and 409 nm for BChl *a* [56,57,58]. In the proteins, the absorption spectra in the *Q* region become quite heterogeneous, with the main peak between 660 and 680 nm [59].

Thus, even if the calculations qualitatively reproduce the difference between the spectra of Chl and BChl, there is a quite large difference in the calculated and the experimental values. However, this is quite normal in calculations like the present one. Our calculated spectra are similar to those obtained in earlier investigations with similar models [50]. Part of the discrepancy comes from the truncation of the side chains. With all side chains, the strongest peaks are found at 631 and 439 nm for Chl *a*, 642 and 525 nm for Chl *b*, and 701 and 352 nm for BChl *a*, i.e. appreciably closer to the experimental values and reproducing the qualitative differences between the three forms of chlorophyll. Moreover, the absolute band positions are not interesting, because we are only interested in how the bands are shifted when axial ligands are added, and such calculated spectral shifts are normally much more accurate than the absolute values. For example, when the Asn axial ligand is added, the *Q* and *B* bands shift by 5 and 3 nm both with and without the chlorophyll side chains.

The shifts in the absorption wavelength and intensities when axial ligands are added to Chl and BChl are listed in Table 9. It can be seen that the absorption wavelength (λ) for both the *Q* and *B* bands increase when an axial ligand is added to the Chl model. The negatively

charged species (Asp, Phos, and Ser^-) give the largest shifts (28–35 nm for the *B* band and 9–19 nm for the *Q* band). The oscillator strengths (*f*) of the *B* bands decrease for all the ligands, whereas the effect on the *Q* band varies. Thus, the spectra of Chl resemble more the experimental ones when axial ligands are added, which has been noted before (with water) [8].

Upon addition of axial ligands to BChl, the *Q* band is in general blue-shifted, except for Met, but only by 1–8 nm. All the oscillator strengths decrease. For the *B* band, all axial ligands increase the absorption wavelength, whereas the oscillator strengths decrease for all ligands, except the neutral oxygen ligands Asn, H_2O, Backb and Ser.

In PSI, most of the chlorophylls absorb at 660–680 nm [59]. However, a few Chl have peaks at 702–708 nm, i.e. above that of the reaction centre (P700). These so called red chlorophylls, have been much discussed [8,15,59,60]. Our calculations show that axial ligation alone cannot explain the large spectral change of these chlorophylls. Instead, they are most likely caused by other interactions with the surrounding protein residues and the formation of dimers and higher multimers of chlorophylls [15].

We have calculated also the spectra of the P700 and P680 dimers. As can be seen from Table 9, the P700 model has a red-shifted *Q* band by 13 nm, in accordance with the observed red-shifted spectrum with a maximum around 700 nm, although the calculated shift is smaller than the experimental one. On the other hand, the P680 model has a slightly blue-shifted *Q* band (by 3 nm), which is in accordance with the fact that it experimentally has a lower absorbance maximum (~680 nm) than P700, although it should still have been red-shifted compared to an isolated Chl molecule. Thus, we can conclude that some of the characteristics of the reaction centres are reproduced by calculations on isolated His-ligated dimers, but not all.

Finally, we have also studied the spatial distribution of axial ligands in three crystal structures, viz those of PSI, PSII, and the LHC (i.e. those shown in the survey in Table 1) [4,5,6]. The results are shown in Figure 4. It can be seen that for PSI and PSII, there is no

clear ordering of the axial ligands, except in the RC. However, the LHC shows some symmetry regarding the spatial distribution of axial ligands, with His ligands mostly in the centre of the complexes, and Asp or Glu immediately outside. It has been proposed that two chlorophylls are the gate to further energy transport from the LHC to neighbouring LHC or an RC [4]. It is worth noting that one of these chlorophylls is ligated by a 1,2-palmistry's-polyphosphates-glycerol, which corresponds to a Phos ligand in our investigation. This ligand has the largest red-shift of all the investigated ligands (+19 nm). This increase in absorption wavelength renders this chlorophyll more favourable as a terminal transmitter in lowering its absorption energy.

Conclusions

We have in a systematic way studied the effect of axial ligation (by water, His, Asp/Glu, Asn/Gln, Met, Ser, Tyr, back-bone, or phosphate) on Chl and BChl. The results show that the axial ligation has relative small effects on the geometry of the chlorophylls and their cation and anion radicals. However, the binding energies in Table 6 show that the first axial ligand binds with a similar strength as the same ligands to haem or vitamin B_{12} complexes. On the other hand, a second axial ligand binds very weakly. This is in accordance with a survey of the axial ligation of chlorophylls in PSI, PSII, and the LHC (Table 1): The great majority of the chlorophylls have a single axial ligand. However, a signification portion (17%) of the chlorophylls have no obvious ligand in PSII, but this is most certainly connected with the low resolution of that structure (350 pm) and the fact that no water molecules are recognized there: In the other two structures, 18–29% of the chlorophylls are ligated by water molecules. Therefore, it is likely that a more accurate structure of PSII will show a similar low frequency of unligated chlorophylls as the other two structures, 0–2%. Moreover, it is possible that even these few sites will turn our to have weakly bound water ligands, if the resolution is increased; the two sites without any axial ligands in PSI are close to the surface of the protein (Figure 4b), where disordered water molecules are most likely to be found.

In view of this, it is quite surprising that the great majority of the previous quantum mechanical studies have modelled chlorophylls without any axial ligands [8,9,10,11]. The reason for this is probably the size of the systems, in combination with the variation of the axial ligand. However, our results clearly show that this is not a good approximation. It has also recently been noted that calculated chlorophyll spectra are closer to experiments if five-coordinate models are employed [8].

There is a clear trend in reduction potentials and BDEs among the ligands, especially in a protein-like environment, viz. Met > H_2O, Ser, Tyr > Asn, His, Backbone > charged residues. This trend may have importance for the fine tuning of potentials and the stability of the complexes.

Finally, we have studied the effect of axial ligand on the main peaks of the absorption spectra of Chl and BChl. The results in Table 9 shows that the axial ligands have some effect (up to 35 nm), red-shifting the *B* band in BChl and both bands for Chl. However, the effect is not enough to explain the occurrence of "red" chlorophylls in PSI. On the other hand, there are at least some correlation between the axial ligation and the position of the chlorophylls in the LHC. In particular, the intrinsic potential of the of the second molecule in the electron-transfer path is always lower than that of the third one, a feature that may prevent the back-transfer of the electron.

Acknowledgements

This investigation has been supported by grants from the Swedish research council and by computer resources of Lunarc at Lund University.

References

1. Brettel K (1997) Biochim Biophys Acta 1318:322-373
2. Kaim W, Schwederski B (1994) Bioinorganic chemistry: Inorganic elements in the chemistry of life. J Wiley & Sons, Chichester, pp 56-78
3. Nilsson A, Dalibor S, Drakenberg T, Spangfort DM, Forsén S, Allen FJ (1997) J Biol Chem 272:18350–18357
4. Liu ZF, Yan HC, Wang KB, Kuang TY, Zhang JP, Gui LL, An XM, Chang WR (2004) Nature 428:287-292
5. Jordan P, Fromme P, Witt HT, Klukas O, Saenger W, Krauss N (2001) Nature 411:909-917
6. Ferreira KN, Iverson TM, Maghlaoui K, Barber J, Iwata S (2004) Science 303:1831-1838
7. Brettel K, Leibl W (2001) Biochim Biophys Acta 1507:100-114
8. Linnanto J, Korppi-Tommola J (2006) Phys Chem Chem Phys 8:663-687
9. Linnanto J, Korppi-Tommola J (2004) J Phys Chem A 108:5872-5882
10. Hasegawa J, Ozeki Y, Ohkawa K, Hada M, Nakatsuji H (1998) J Phys Chem B 102:1320-1326
11. Sundholm D (1999) Chem Phys Lett 302:480-484
12. Thompson MA, Schenter GK (1995) J Phys Chem 99:6374-6386
13. Linnanto J, Korppi-Tommola JEI Helenius VM (1999) J Phys Chem B 103:8739-8750
14. Ihalainen JA, Linnanto J, Myllyperklio P, van Stokkum IHM, Ücker B, Scheer H, Korppi-Tommola JEI (2001) J Phys Chem B 105:9849-9856
15. Damjanovic A, Vaswani HM, Fromme P, Fleming GR (2002) J Phys Chem B 106:10251-10262
16. Blomberg MRA, Siegbahn PEM, Babcock GT (1998) J Am Chem Soc 120:8812-8824
17. Hutter MC, Hughes, JM, Reimers JR, Husoh NS (1999) J Phys Chem B 103:4906-4915
18. Zhang XD, Ma SH, Wang YN, Zhang XK, Zhang QY (2000) J Pch P 131:85-94
19. Zhang XD, Zhang CX, Ma SH, Xu H, Shen LL, Li LB, Zhang XK, Kuang TY, Zhang QY (2001) Acta Chim 59:456-465
20. Crystal J, Friesner RA (2000) J Phys Chem A 104:2362-2366
21. Sinnecker S, Koch W, Lubitz W (2000) PCCP 2:4772:4778
22. O'Malley PJ, Cullins SJ (2001) J Am Chem Soc 123:11042-11046
23. Datta SN, Parandekar PV, Lochan RC (2001) J Phys Chem B 105:1442-1451
24. Linnanto J, Korppi-Tommola JEI (2002) PCCP 4:3453-3460
25. Ivashin N, Larsson S (2002) J Phys Chem B 106:3996-4009
26. Sun YM, Wang HZ, Zhao FL, Sun JZ (2004) Chem Phys Lett 387:12-16
27. He Z, Sundström V, Pullerits T (2002) J Phys Chem B 106:11606-11612
28. Sundholm D (2003) PCCP 5:4265-4271
29. Loll B, Kern J, Saenger W, Zouni A, Biesiadka J (2005) Nature 438:1040-1044
30. Becke AD (1988) Phys Rev A 38:3098-3100
31. Perdew JP (1986) Phys Rev B 33:8822-8824
32. Hehre WJ, Radom L, Schleyer PvR, Pople JA (1986) Ab initio molecular orbital theory. Wiley-Interscience, New York
33. Eichkorn K, Treutler O, Ohm H, Haser M, Ahlrichs R (1995) Chem Phys Lett 240:283–289
34. Eichkorn K, Weigend F, Treutler O, Ahlrichs O (1997) Theor Chem Acc 97:119-124
35. Hertwig RH, Koch W (1997) Chem Phys Lett 268:345-351
36. Klamt A, Schüürmann G (1993) J Chem Soc Perkin Trans 2:799-805
37. Schäfer A, Klamt A, Sattel D, Lohrenz JCW, Eckert F (2000) PCCP 2:2187-2193
38. Sharp KA, Honig B (1990) Annu Rev Biophys Biophys Chem 19:301-332
39. Honig B Nicholls A (1995) Science 268:1144-1149
40. Klamt A, Jonas V, Bürger T, Lohrenz JCW (1998) J Phys Chem 102:5074-5085
41. Reiss H, Heller A (1985) J Phys Chem 89:4207-4213
42. Bauernschmitt R, Ahlrichs R (1996) Chem Phys Lett 256:454-464

43. Dreuw A, Head-Gordon M (2005) Chem Rev 105:4009-4037
44. Schäfer A, Huber C, Ahlrichs R (1994) J Chem Phys 100:5829-5835
45. Linnanto J Korppi-Tommola J (2004) J Phys Chem A 108:5872-5882
46. Seda J, Burda JV, Brázdová V, Kapsa V (2004) Int J Mol Sci 5:196-213
47. Dahlbom MG, Reimers JR (2005) Mol Phys 103:1057-1065
48. Hersleth H-P, Ryde U, Rydberg P, Görbitz CH, Andersson KK (2006), J Inorg Biochem, 100:460-476
49. Amzel LM (1997) Proteins Struct Funct Gen 28:144-149
50. Jensen KP, Ryde U (2003) J Phys Chem B 107:7539-7545
51. Jensen KP, Ryde U (2005) J Porph Phthalocyanines 9:581-606
52. Shen Y, Ryde U (2004) J Inorg Biochem 98:878-895
53. Jensen KP, Ryde U (2003) ChemBioChem, 4:413-424
54. Watanabe T, Kobayashi M, in Chlorophylls, ed Scheer H, CRC Press, Boca Raton, Fl, 1991, p 287
55. Hasegawa K, Noguchi T (2005) Biochem 44:8865-8872
56. Strain HH, Thomas MR, Katz JJ (1963) Biochim Biophys Acta 75:306-311
57. Houssier C, Sauer K (1970) J Am Chem Soc 92:779-791
58. Hoff AJ, Amesz J, in Chlorophylls, ed Scheer H, CRC Press, Boca Raton, Fl, 1991, p 723
59. Gobets B, van Stokkum IHM, Rogner M, Kruip J, Schlodder E, Karapetyan ENV, Dekker JP, van Grondelle R (2001) Biophys J 81:407-424
60. Zazubovich V, Matsuzaki S, Johnson TW, Hayes JM, Chitnis PR, Small GJ (2002) Chem Phys 275:47-59

Table 1. A survey of axial ligands in three crystal structures of the photosynthetic complexes, listing the frequency (%) and Mg–ligand distance range (pm).

Ligand	LHC[a]		PSI[b]		PSII[c]	
	Frequency	Range	Frequency	Range	Frequency	Range
No	0		2		17	
Met			2	255-260		
Tyr			1	244		
Water	29	187-214	18	195-250		
Alcohol	7	339-370			3	342-343
Asn/Gln	14	214-232	4	210-218	3	226-228
Back-bone	14	211-222	1	224	3	347-348
His	14	219-232	68	217-275	75	223-232
Phosphate	7	224-236	1	226		
Asp/Glu	21	207-222	3	214-277		
Ethyl					3	246

[a] The LHC in spinach at 287 pm resolution, with 140 chlorophylls, PDB file 1RWT [4].

[b] Photosystem I from *Synechococcus elongatus* at 250 pm resolution, with 96 chlorophylls, PDB file 1JB0 [5].

[c] Photosystem II from *Thermosynechococcus elongatus* at 350 pm resolution, with 72 chlorophylls, PDB file 1S5L [6].

[d] The phosphate group in 1,2-palmistry's-polyphosphates-glycerol.

[e] Serine in 1S5L, (1R,3R)-6-{(3E,5E,7E,9E,11E,13E,15E,17E)-18-[(1S,4R,6R)-4-hydroxy-

2,2,6-trimethyl-7-oxabicyclo[4.1.0]hept-1-yl]-3,7,12,16-tetramethyloctadeca-1,3,5,7,9,11,13,15,17-nonaenylidene}-1,5,5-trimethylcyclohexane-1,3-diol (in addition to water) in 1RWT.

[f] The ethyl group of another chlorophyll molecule, together with a His ligand on the opposite side. This is most likely an artefact of the low resolution of this structure. In a newer structure of the same protein [29], the Mg–C distance is ~498 pm.

Table 2. Mg–ligand distances (pm) for the the optimised Chl structures (pm). Oop is the distance of the Mg ion out of the average porphyrin plane (pm).

Ligand	N1	N2	N3	N4	Ligand	Oop
No	203.7	208.1	202.5	216.6		0.0
Met	205.8	210.3	204.9	219.7	273.6	28.4
Tyr	206.6	210.1	203.9	219.4	220.4	26.1
H_2O	205.1	211.5	205.6	217.9	216.7	26.0
Ser	205.6	212.0	205.3	218.1	215.8	28.4
Asn	207.0	211.7	206.5	221.9	210.2	39.1
Backb	207.2	212.0	206.6	221.6	209.7	39.9
His	207.2	212.2	206.2	220.8	221.0	37.7
2His	206.4	211.5	205.4	217.8	234.6, 234.6	0.0
Phos	211.0	216.5	209.9	223.4	199.4	57.7
Asp	212.0	218.0	211.1	225.8	198.5	63.0
Ser^-	213.4	218.4	212.5	229.1	190.2	68.1

Table 3. Change in the Mg–ligand distances (pm) for the Chl cation and anion radicals. Oop is the distance of the Mg ion out of the average porphyrin plane (pm).

Ligand	Cation Radical						Anion Radical					
	N1	N2	N3	N4	Ligand	Oop	N1	N2	N3	N4	Ligand	Oop
No	-0.6	-0.7	-0.3	-1.3		0.1	1.6	0.2	1.8	1.1		0.0
Met	0.9	1.0	0.3	0.4	-5.4	8.2	1.1	-1.0	0.9	-2.1	7.1	-7.4
Tyr	0.6	0.8	1.0	0.7	-4.8	10.8	3.6	-1.1	0.1	-3.2	14.9	-8.3
H_2O	1.2	-0.2	-0.5	1.4	-3.7	9.2	0.6	1.6	2.1	-2.8	5.6	-5.0
Ser	1.2	-0.4	0.0	1.4	-3.4	8.9	1.0	1.6	1.0	-2.8	6.0	-5.2
Asn	1.2	1.0	0.3	0.8	-4.7	7.5	0.8	-0.6	0.9	-3.2	5.3	-6.6
Backb	1.3	1.1	0.4	1.1	-4.7	8.0	0.8	-0.9	0.8	-2.5	4.9	-7.0
His	1.3	0.8	0.5	1.3	-3.0	8.4	0.9	-0.4	0.9	-2.8	3.7	-7.5
2His	0.3	-0.3	0.0	1.2	-3.2, -3.2	0.0	1.5	0.3	1.7	-1.0	1.3, 1.3	0.0
Phos	0.1	-0.3	-0.8	0.1	-3.1	0.7	2.1	-0.6	1.5	-1.9	3.7	-2.5
Asp	-1.7	-2.4	-1.1	-0.3	1.3	-5.2	2.0	-0.5	1.6	1.6	1.9	-2.6
Ser^-	-3.7	-3.7	-3.7	-5.0	7.5	-15.4	2.2	-0.1	2.1	-1.0	3.4	-1.0

Table 4. Mg–ligand distances (pm) for the the optimised BChl structures (pm). Oop is the distance of the Mg ion out of the average porphyrin plane (pm).

Ligand	N1	N2	N3	N4	Ligand	Oop
No	203.1	214.7	201.9	217.6		0.0
Met	205.0	216.5	204.1	220.5	272.7	27.1
Tyr	204.3	216.8	205.0	219.5	219.6	24.7
H_2O	204.6	217.9	204.6	219.0	215.8	25.6
Ser	204.8	217.3	205.0	219.7	216.7	27.7
Asn	206.3	218.1	205.6	222.1	210.2	37.9
Backb	206.4	218.3	205.6	222.1	209.5	38.7
His	206.5	218.8	205.3	221.4	221.2	36.8
2His	205.8	217.0	205.3	219.6	232.0, 231.8	0.4
Phos	210.2	222.6	209.2	223.2	198.5	56.8
Asp	211.3	224.8	210.6	226.4	198.8	63.4
Ser^-	212.5	224.9	211.6	228.9	190.4	67.0

Table 5. Change in the Mg–ligand distances (pm) for the BChl cation and anion radicals. Oop is the distance of the Mg ion out of the average porphyrin plane (pm).

Ligand	Cation Radical						Anion Radical					
	N1	N2	N3	N4	Ligand	Oop	N1	N2	N3	N4	Ligand	Oop
No	-0.8	-1.1	-0.5	-1.3		0.0	1.6	-0.9	2.0	-1.2		0.0
Met	0.3	0.6	0.5	-0.3	-4.6	9.1	1.1	-2.2	1.4	-1.8	7.3	-6.5
Tyr	0.6	0.5	0.2	0.3	-4.1	10.6	0.1	-2.6	4.1	-2.8	13.3	42.4
H_2O	0.4	-0.7	-0.3	0.8	-3.1	8.6	0.4	-0.4	3.2	-3.1	6.6	-4.9
Ser	0.5	-0.1	-0.3	0.8	-5.3	8.7	0.5	-2.9	4.0	-1.7	4.8	-4.5
Asn	0.4	0.5	0.5	0.1	-4.3	7.7	1.0	-1.9	1.6	-2.7	4.6	-5.5
Backb	0.5	0.6	0.7	0.3	-4.3	8.3	0.8	-2.2	1.5	-2.5	4.8	-6.4
His	0.5	0.3	0.8	0.6	-2.7	9.0	0.8	-1.9	1.3	-2.8	3.0	-7.8
2His	-0.6	-1.2	-0.6	-1.2	-0.2, -0.0	-0.2	1.3	-0.9	2.1	-0.8	1.1, 1.3	-0.4
Phos	-0.6	-1.0	-0.5	-0.5	-2.8	-1.6	2.0	-1.8	2.6	0.6	3.6	0.1
Asp	-1.6	-2.4	-1.1	-2.8	-0.2	-3.2	1.9	-2.2	2.0	-2.2	1.7	-3.3
Ser^-	-2.5	-2.9	-2.5	-3.6	4.0	-7.4	2.2	-0.9	2.9	-1.5	3.5	-0.4

Table 6. BDEs (kJ/mole) of the various axial ligands to Chl and BChl in continuum solvents with different values for the dielectric constant (?).

Axial ligand	Chlorophyll			Bacterial Chlorophyll		
	ε = 1	ε = 4	ε = 80	ε = 1	ε = 4	ε = 80
Met	27.7	19.7	16.1	31.3	21.9	17.2
Tyr	35.7	22.2	15.1	39.4	24.9	17.0
H_2O	47.2	35.7	29.6	48.9	39.2	34.2
Ser	49.7	39.3	34.0	49.1	40.1	35.4
Asn	61.6	55.5	52.5	67.3	59.3	54.9
Backb	67.5	58.1	52.9	71.2	60.3	54.1
His	69.7	61.5	57.0	67.3	60.9	57.6
2His	84.3	61.1	47.3	98.9	71.4	54.7
Phos	170.0	87.4	47.5	178.9	98.4	58.5
Asp	189.9	101.7	61.8	191.9	104.7	65.1
Ser^-	259.6	153.0	105.2	265.0	158.2	109.7

Table 7. Reduction potentials (V) of the Chl and BChl cation radicals in continuum solvents with different values for the dielectric constant (?).

Axial ligand	Chlorophyll			Bacterial Chlorophyll		
	ε = 1	ε = 4	ε = 80	ε = 1	ε = 4	ε = 80
No	2.09	1.11	0.64	1.60	0.64	0.18
Met	1.88	0.98	0.56	1.41	0.53	0.12
Tyr	1.88	0.97	0.53	1.42	0.53	0.11
H_2O	1.87	0.90	0.49	1.39	0.46	0.02
Ser	1.85	0.91	0.47	1.32	0.43	0.02
Asn	1.63	0.85	0.50	1.19	0.41	0.06
Backb	1.62	0.82	0.46	1.17	0.38	0.03
His	1.68	0.87	0.51	1.20	0.42	0.08
2His	1.51	0.75	0.42	1.05	0.31	-0.02
Phos	-1.01	-0.08	0.39	-1.36	-0.41	0.06
Asp	-0.98	0.07	0.59	-1.44	-0.42	0.08
Ser^-	-1.12	0.02	0.52	-1.45	-0.39	0.12
Pheo	2.18	1.23	0.79			
P700	1.38	0.74	0.44			
P700 No His	1.94	1.09	0.66			
P680	1.51	0.89	0.67			

Table 8. Reduction potentials (V) of Chl and BChl (giving the anion radicals) in continuum solvents with different values for the dielectric constant (?).

Axial ligand	Chlorophyll			Bacterial Chlorophyll		
	ε = 1	ε = 4	ε = 80	ε = 1	ε = 4	ε = 80
No	-2.69	-1.69	-1.18	-2.68	-1.67	-1.16
Met	-2.79	-1.79	-1.29	-2.79	-1.79	-1.29
Tyr	-2.79	-1.84	-1.37	-2.78	-1.84	-1.37
H_2O	-2.79	-1.87	-1.41	-2.81	-1.89	-1.44
Ser	-2.83	-1.84	-1.35	-2.81	-1.83	-1.35
Asn	-2.99	-1.92	-1.38	-3.01	-1.92	-1.36
Backb	-3.03	-1.95	-1.40	-3.04	-1.95	-1.40
His	-3.01	-1.90	-1.33	-3.01	-1.89	-1.32
2His	-3.16	-2.03	-1.45	-3.14	-2.05	-1.49
Phos	-5.43	-2.65	-1.29	-5.48	-2.73	-1.39
Asp	-5.57	-2.82	-1.47	-5.59	-2.85	-1.51
Ser^-	-5.70	-2.82	-1.41	-5.74	-2.85	-1.43
Pheo	-2.58	-1.53	-0.99			
P700	-2.96	-2.07	-1.62			
P700 No His	-2.49	-1.79	-1.45			
P680	-2.79	-1.94	-1.51			

Table 9. Spectral shift for the *Q* and *B* bands of Chl and BChl arising from addition of an axial ligand. ?? is the absorption wavelength (in nm) and *f* is the oscillator strength.

	Chlorophyll				Bacterial Chlorophyll			
Band	*Q*		*B*		*Q*		*B*	
Axial ligand	??	*f*	??	*f*	??	*f*	??	*f*
No	598	0.10	434	0.16	657	0.25	341	0.49
Met	5	=	6	↓	2	↓	11	↓
Tyr	4	=	7	=	-1	↓	6	↓
H_2O	3	↑	8	↓	-3	↓	3	↑
Ser	4	↑	6	↓	-2	↓	4	↑
Asn	3	↑	10	↓	-3	↓	4	↑
Backb	4	↑	10	↓	-2	↓	5	↑
His	5	=	14	=	-2	↓	5	↓
2His	12	↓	9	↓	-2	↓	17	↓
Phos	19	=	33	↓	-1	↓	9	↓
Asp	9	↓	35	↓	-6	↓	12	↓
Ser^-	11	=	28	↓	-8	↓	7	↓
P700	13	↑	6	↓				
P680	-3	↑	3	↑				

Figure 1. The structure of Chl *a*, Chl *b*. and BChl *a*.

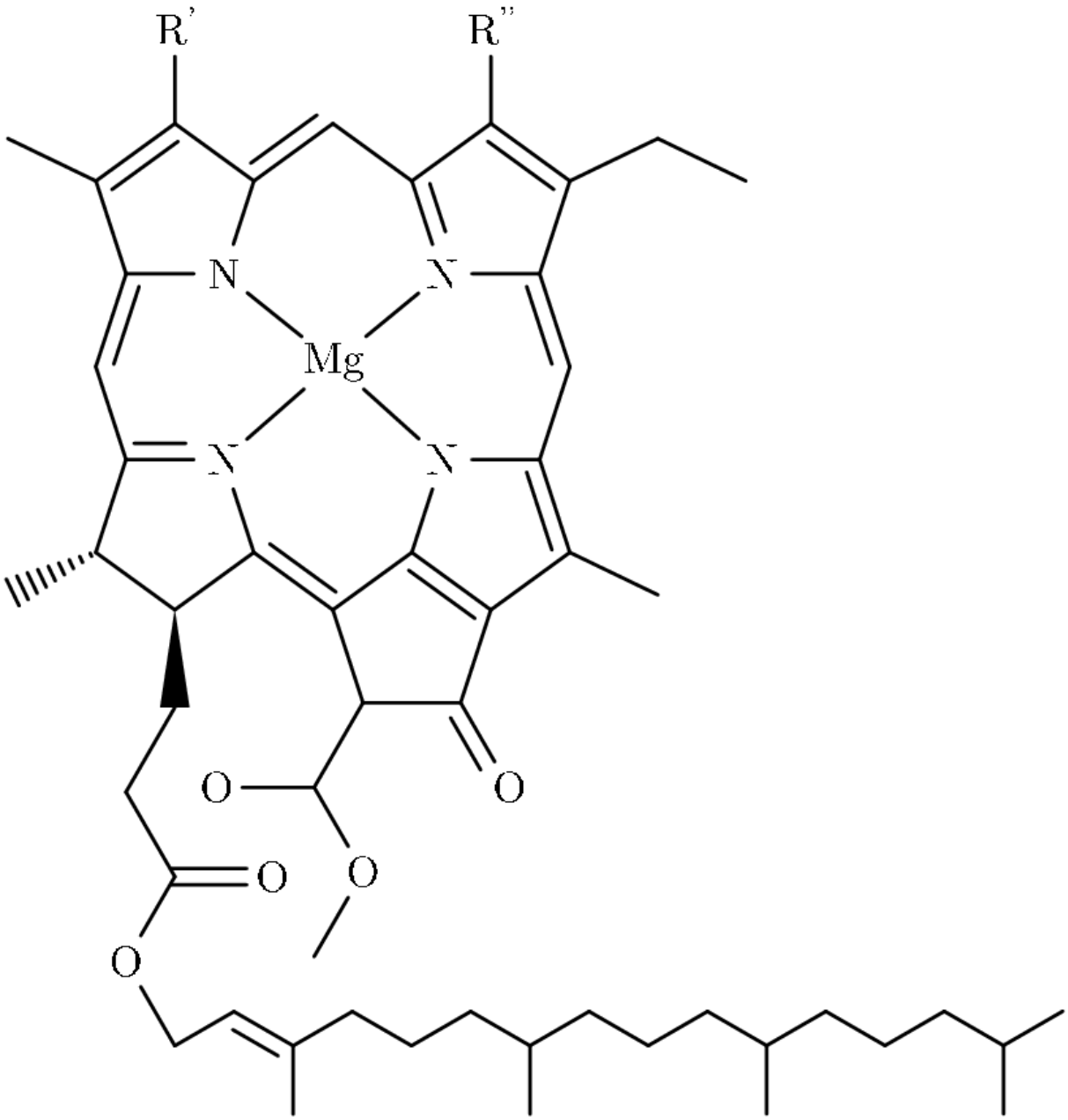

Chl *a*; R' = $-CHCH_2$, R'' = $-CH_3$

Chl *b*; R' = $-CHCH_2$, R'' = $-CHO$

BChl *a*; R' = $-COCH_3$, R'' = $-CH_3$

Figure 2. The model used for (a) Chl and (b) BChl without ligands.

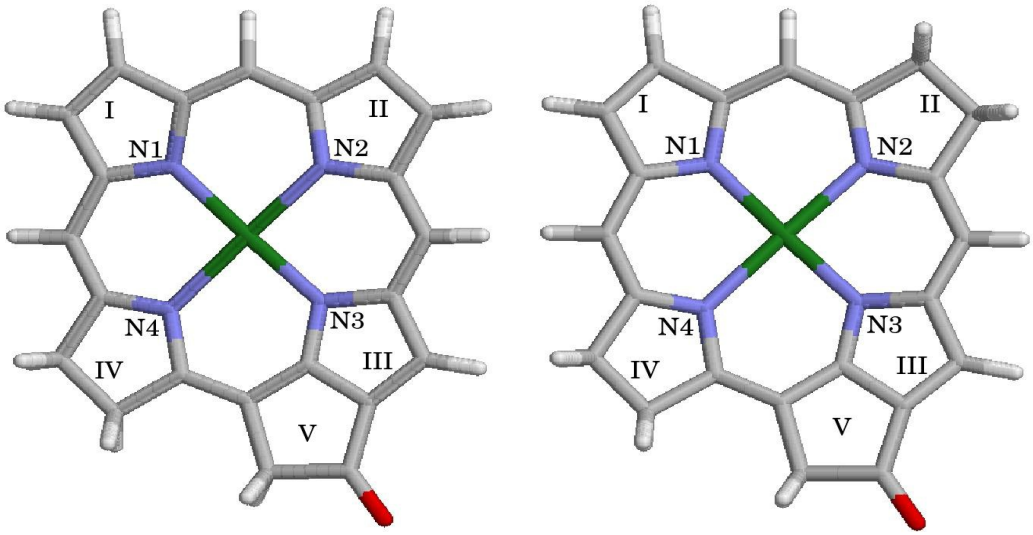

a: Chl b: BChl

Figure 3. The model used for the calculations on P700 and P680 [5,6].

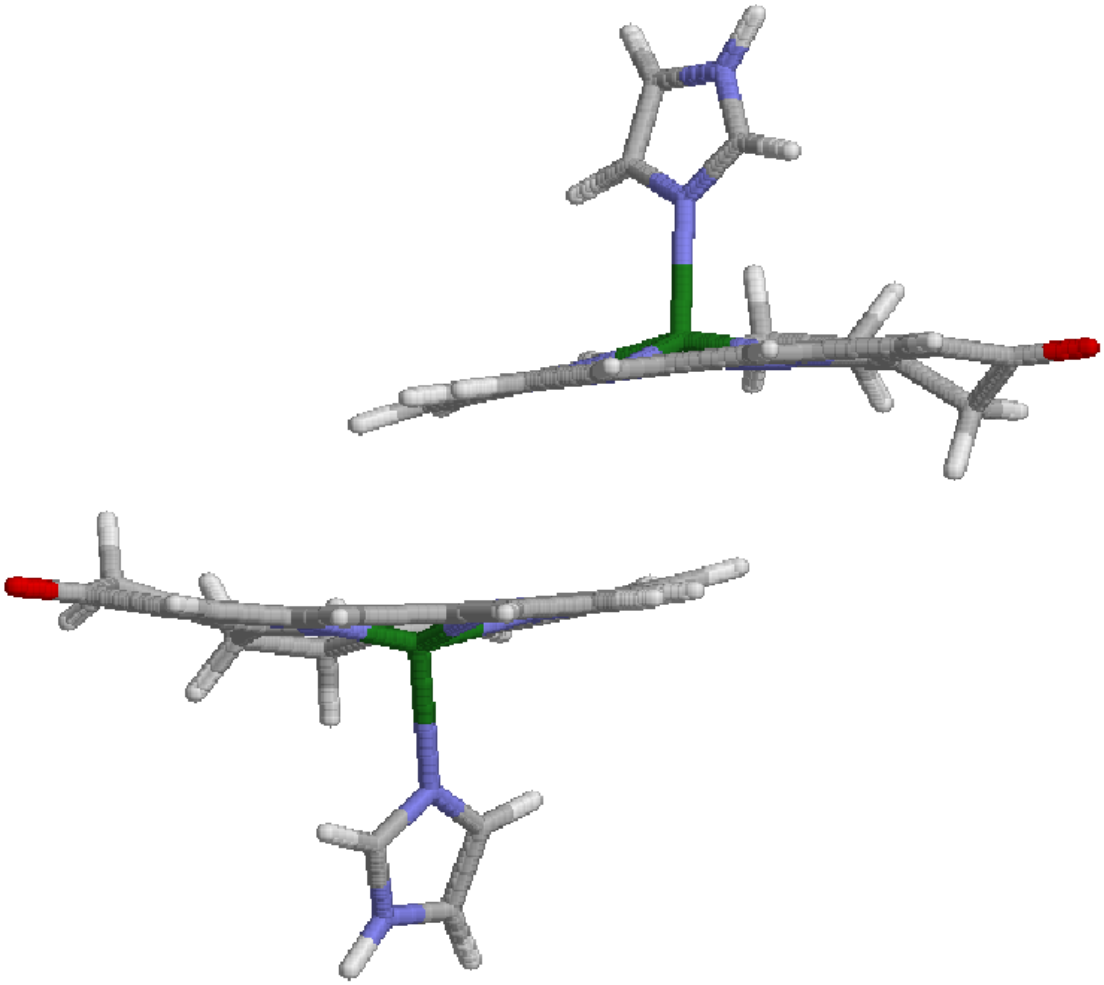

Figure 4. The location of various axial ligands in the crystal structures of LHC (a; only the central core), PSI (b), and PSII (c). The chlorophyll molecules are colour coded after their axial ligand in the following way: no – grey, His – blue, Asp/Glu – red, Asn/Gln – orange, Water – cyan, Met – yellow, back-bone – green, phosphate – magenta, alcohols – brown, Tyr – black.

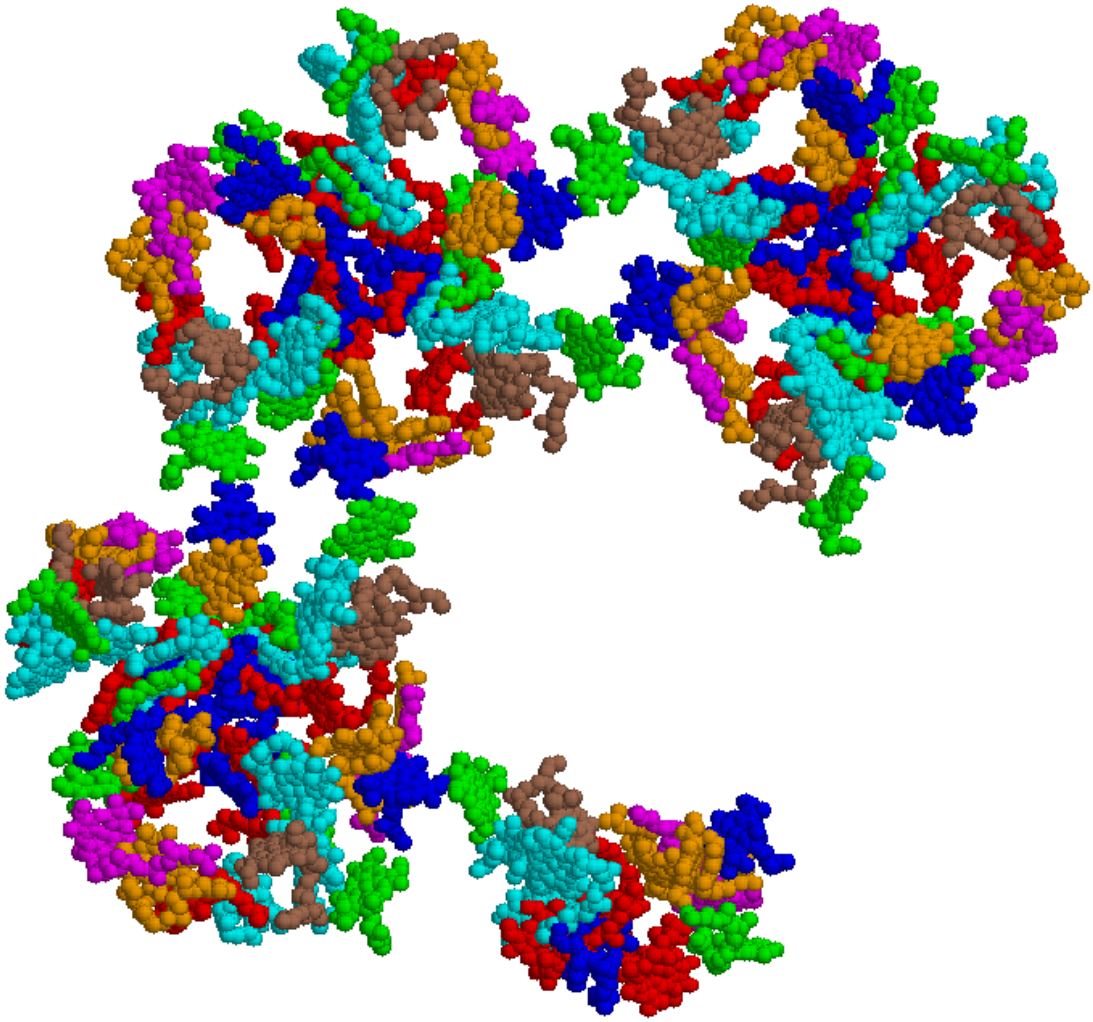

(a) LHC

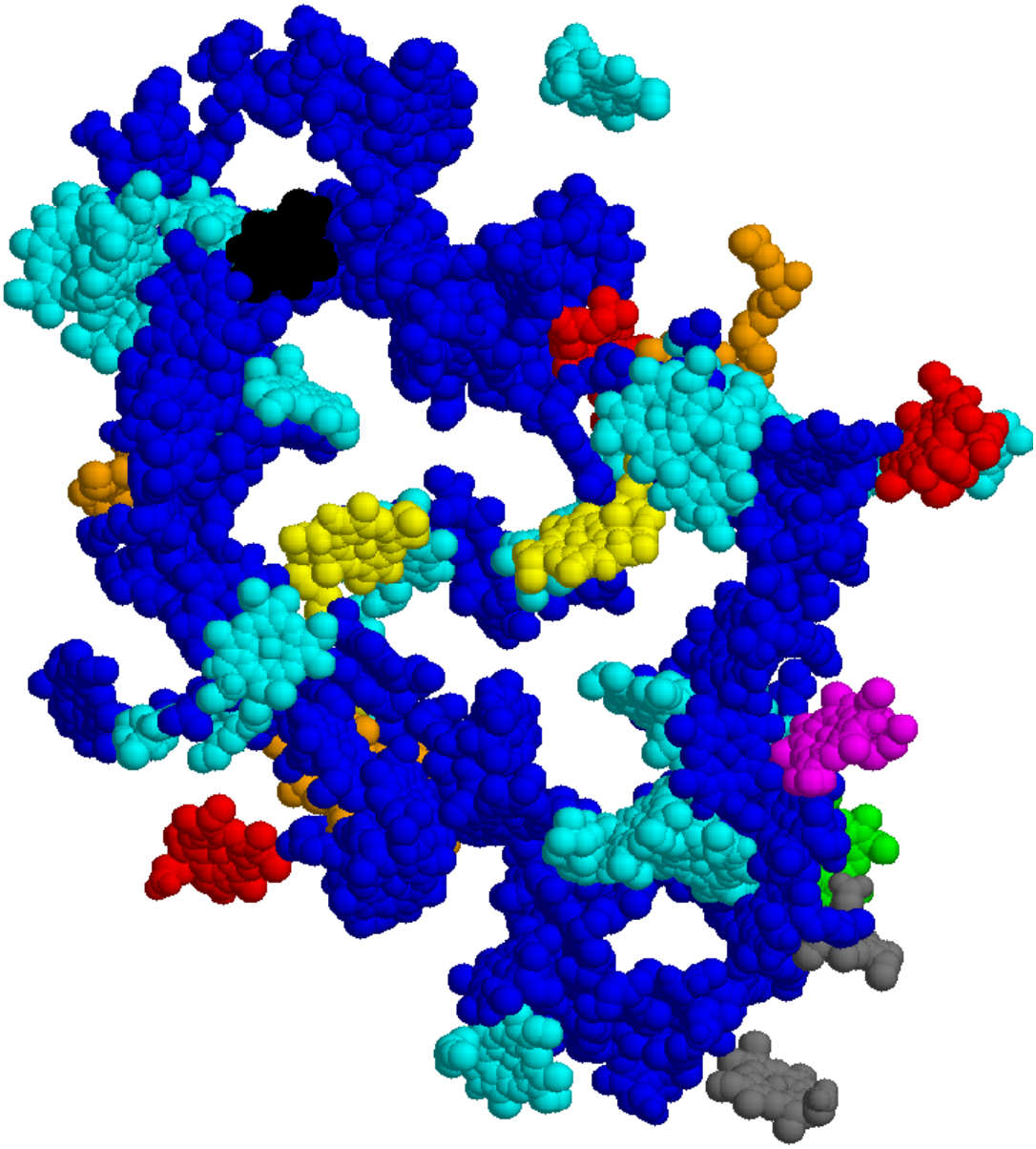

(b) PSI

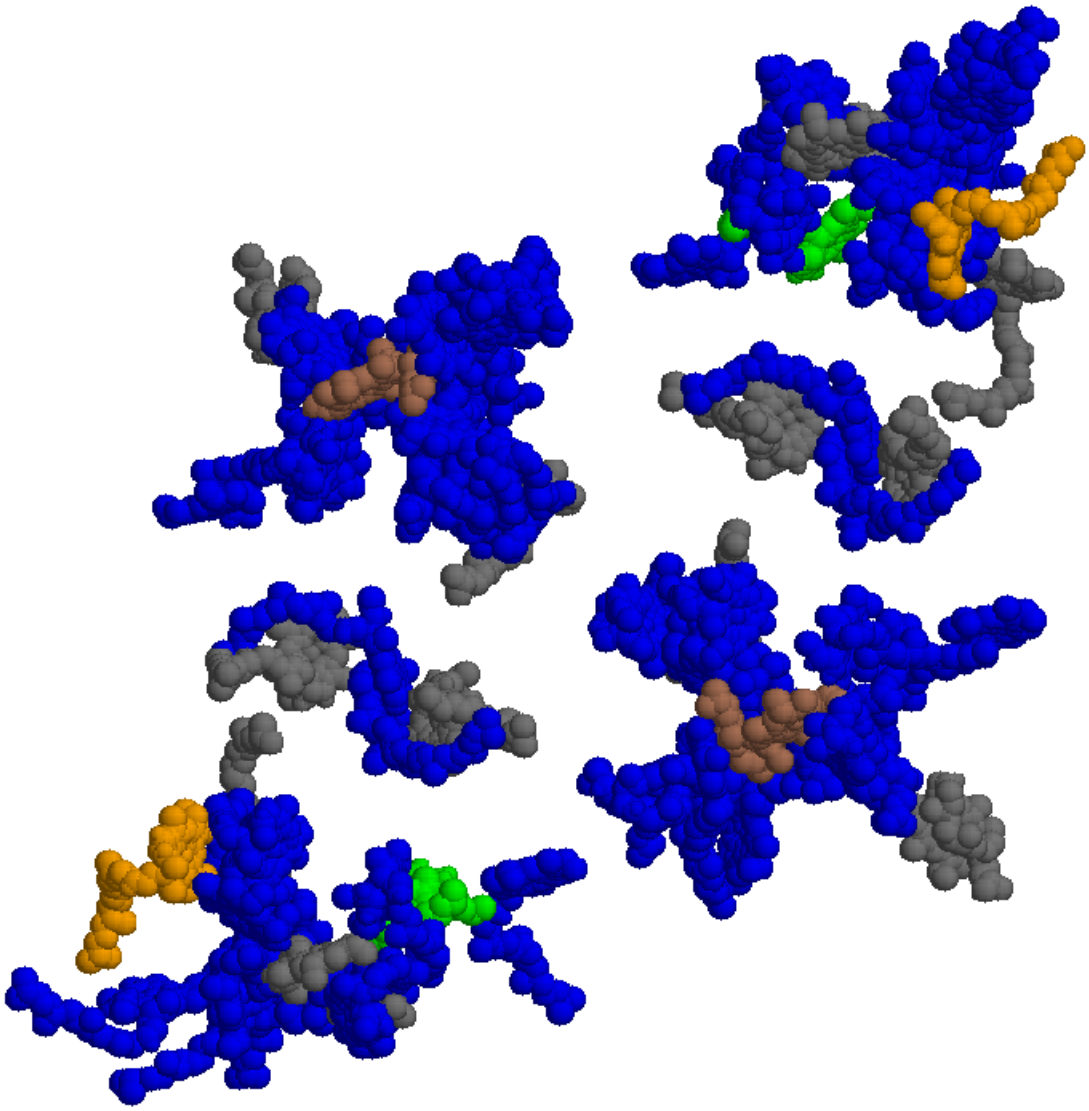

(c) PSII